

Petr Sváček; Jaromír Horáček

Numerical approximation of flow in a symmetric channel with vibrating walls

In: Jan Chleboun and Petr Přikryl and Karel Segeth and Jakub Šístek (eds.): Programs and Algorithms of Numerical Mathematics, Proceedings of Seminar. Dolní Maxov, June 6-11, 2010. Institute of Mathematics AS CR, Prague, 2010. pp. 183–196.

Persistent URL: <http://dml.cz/dmlcz/702758>

**Terms of use:**

© Institute of Mathematics AS CR, 2010

Institute of Mathematics of the Czech Academy of Sciences provides access to digitized documents strictly for personal use. Each copy of any part of this document must contain these *Terms of use*.



This document has been digitized, optimized for electronic delivery and stamped with digital signature within the project *DML-CZ: The Czech Digital Mathematics Library*  
<http://dml.cz>

# NUMERICAL APPROXIMATION OF FLOW IN A SYMMETRIC CHANNEL WITH VIBRATING WALLS\*

Petr Sváček, Jaromír Horáček

## Abstract

In this paper the numerical solution of two dimensional fluid-structure interaction problem is addressed. The fluid motion is modelled by the incompressible unsteady Navier-Stokes equations. The spatial discretization by stabilized finite element method is used. The motion of the computational domain is treated with the aid of Arbitrary Lagrangian Eulerian (ALE) method. The time-space problem is solved with the aid of multigrid method.

The method is applied onto a problem of interaction of channel flow with moving walls, which models the air flow in the glottal region of the human vocal tract. The pressure boundary conditions and the effects of the isotropic and anisotropic mesh refinement are discussed. The numerical results are presented.

## 1 Introduction

This paper is concerned with numerical simulation of unsteady viscous incompressible flow in a simplified model of the glottal region of the human vocal tract with the aid of the finite element method (FEM). The main attention is paid to the efficient computation of the flow field. For the robust and efficient solver both the advanced stabilization (as streamline upwind/Petrov Galerkin stabilizations, cf. [6], [7]) and solution methods (as multigrid and/or domain decomposition, cf. [19], [9], [10], [13]) have to be employed.

FEM is well known as a general discretization method for partial differential equations. It can handle easily complex geometries and also boundary conditions employing derivatives. However, straightforward application of FEM procedures often fails in the case of incompressible Navier-Stokes equations. The reason is that momentum equations are of advection-diffusion type with dominating advection. The Galerkin FEM leads to unphysical solutions if the grid is not fine enough in regions of strong gradients (e.g. boundary layer). In order to obtain physically admissible correct solutions it is necessary to apply suitable mesh refinement (e.g. anisotropically refine mesh, cf. [5]) combined with a stabilization technique, cf. [7], [3], [18], [16].

Furthermore, the time and space discretized linearized problem of the arising large system of linear equations needs to be solved in fast and efficient manner. The

---

\*This research was supported under the Project OC 09019 “Modelling of voice production based on biomechanics” within the program COST of the Ministry of Education of the Czech Republic, under grant No. 201/08/0012 of the Grant Agency of the Czech Republic and the Research Plan MSM 6840770003 of the Ministry of Education of the Czech Republic.

application of direct solvers as UMFPACK (cf. [4]) leads to robust method, where different stabilizations procedures can be easily applied even on anisotropically refined grids. However, the application of direct solver for system of equations with more than approximately  $10^5$  unknowns becomes unfeasible in many cases (depending on computer CPU and memory).

In that case the application of multigrid (cf. [19]) or domain decomposition methods is an option, cf. [13]. In this paper a simplified version of multigrid method is shortly described together with a choice of finite elements and stabilization procedures. Even when the method is simplified, it was found to be efficient and robust enough.

The developed method is applied to the numerical solution of a channel flow modelling the glottis region of the human vocal tract including the vibrating vocal folds. The vibrations of the channel wall are prescribed, see [14]. Further, in order to obtain physically relevant results the pressure drop boundary conditions are employed, cf. [8].

First the mathematical model consisting of time dependent computational domain and incompressible flow model. Further, in Section 3 the time and space discretization is described and Section 4 describes the application of a simple multigrid version. Section 5 shows the numerical results.

## 2 Mathematical model

The model problem consists of flow model, which describes the fluid motion in the time-dependent computational domain  $\Omega_t$ , i.e. in a channel with moving walls, see Fig. 1. For the description and the approximation on moving meshes the Arbitrary Lagrangian-Eulerian (ALE) method is employed, cf. [12]. The geometry of the channel is chosen according [14], where a different distance between the moving walls, i.e. the gap  $g(t)$ , was considered. Further, on the outlet part of the channel a modification of do-nothing boundary condition was applied in order to allow the vortices flow smoothly out of the computational domain. On the inlet either the Dirichlet boundary condition for velocity is prescribed or preferably we use the pressure drop formulation, similarly as in cf. [8]. The presented mathematical model (and also its numerical approximation) is a slight modification of the mathematical model applied to the numerical simulation of flow induced airfoil vibrations in our previous works, cf. [18].

### 2.1 Arbitrary Lagrangian Eulerian method

In order to treat the fluid flow on moving domains, the so-called Arbitrary Lagrangian Eulerian method is used. We assume that  $\mathcal{A} = \mathcal{A}(\xi, t) = \mathcal{A}_t(\xi)$  is an ALE mapping defined for all  $t \in (0, T)$  and  $\xi \in \Omega_0$ , which is smooth enough and continuously differentiable mapping of  $\Omega_0$  onto  $\Omega_t$ . We define the *domain velocity*  $\mathbf{w}_D : \mathcal{M} \rightarrow R$  satisfies

$$\mathbf{w}_D(\mathcal{A}(\xi, t), t) = \frac{\partial \mathcal{A}}{\partial t}(\xi, t) \quad \text{for all } \xi \in \Omega_0 \text{ and } t \in (0, T). \quad (1)$$

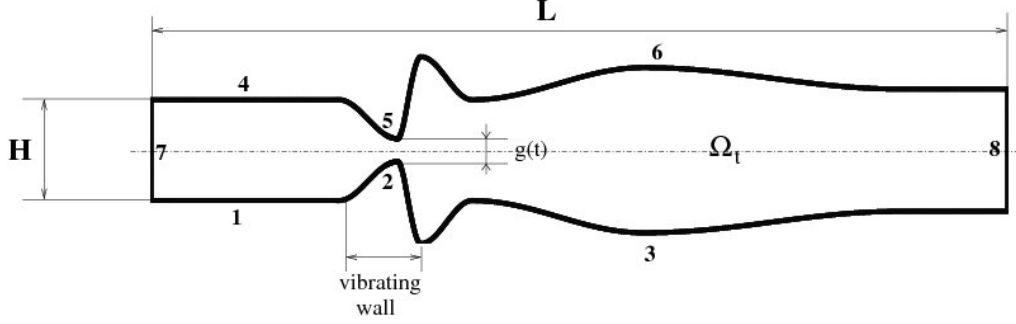


**Fig. 1:** Computational domain and boundary parts: The inlet part of the boundary  $\Gamma_I$  (number 7), the outlet part of the boundary  $\Gamma_O$  (number 8), the fixed walls  $\Gamma_D$  (numbers 1,4,3,6) and vibrating walls  $\Gamma_{Wt}$  (numbers 2, 5).

Furthermore the symbol  $D^A/Dt$  denotes the ALE derivative, i.e. the time derivative with respect to the reference configuration. The ALE derivative satisfies (cf. [18], [11])

$$\frac{D^A f}{Dt}(x, t) = \frac{\partial f}{\partial t}(x, t) + \mathbf{w}_D(x, t) \cdot \nabla f(x, t). \quad (2)$$

In the present paper the ALE mapping can be analytically prescribed, but in the future this mapping will be a part of solution similary as in cf. [18].

## 2.2 Flow model

Let us consider the following system of the incompressible Navier-Stokes equations in a bounded time-dependent domain  $\Omega_t \subset R^2$  written in ALE form

$$\begin{aligned} \frac{D^A \mathbf{v}}{Dt} - \nu \Delta \mathbf{v} + ((\mathbf{v} - \mathbf{w}_D) \cdot \nabla) \mathbf{v} + \nabla p &= 0, & \text{in } \Omega_t, \\ \nabla \cdot \mathbf{v} &= 0, & \text{in } \Omega_t, \end{aligned} \quad (3)$$

where  $\mathbf{v} = \mathbf{v}(x, t)$  is the flow velocity,  $p = p(x, t)$  is the kinematic pressure (i.e. pressure divided by the constant fluid density  $\rho_\infty$ ) and  $\nu$  is the kinematic viscosity.

The boundary of the computational domain  $\partial\Omega_t$  consists of mutually disjoint parts  $\Gamma_D$  (wall),  $\Gamma_I$  (inlet),  $\Gamma_O$  (outlet) and the moving part  $\Gamma_{Wt}$  (oscillating wall). The following boundary conditions are prescribed

$$\begin{aligned} \text{a) } \mathbf{v}(x, t) &= \mathbf{0} & \text{for } x \in \Gamma_D, \\ \text{b) } \mathbf{v}(x, t) &= \mathbf{w}_D(x, t) & \text{for } x \in \Gamma_{Wt}, \\ \text{c) } -(p - p_{ref}^o) \mathbf{n} + \frac{1}{2}(\mathbf{v} \cdot \mathbf{n})^- \mathbf{v} + \nu \frac{\partial \mathbf{v}}{\partial \mathbf{n}} &= 0, & \text{on } \Gamma_O, \\ \text{d) } -(p - p_{ref}^i) \mathbf{n} + \frac{1}{2}(\mathbf{v} \cdot \mathbf{n})^- \mathbf{v} + \nu \frac{\partial \mathbf{v}}{\partial \mathbf{n}} &= 0, & \text{on } \Gamma_I, \end{aligned} \quad (4)$$

where  $\mathbf{n}$  denotes the unit outward normal vector, the constants  $p_{ref}^i, p_{ref}^o$  denotes the reference pressure values, and  $\alpha^-$  denotes the negative part of a real number  $\alpha$ . In computations the condition (4d) can be replaced by the condition

$$\text{e) } \mathbf{v}(x, t) = \mathbf{v}_D \quad \text{for } x \in \Gamma_I. \quad (5)$$

Finally, we prescribe the initial condition

$$\mathbf{v}(x, 0) = \mathbf{v}^0(x) \quad \text{for } x \in \Omega_0.$$

### 3 Numerical approximation

In this section the numerical approximation of the mathematical model given in Section 2 is shown. As already mentioned the presented numerical approximation is a slight modification of our previous works, cf. [18], [17]. Nevertheless there are several significant differences, which were found to be important for the numerical approximation: boundary conditions used on the inlet/outlet part of the computational and its weak formulation, a modified Galerkin/Least-Squares (GLS) scheme employed for stable pair of finite elements, and the choice of stabilizing parameters. The space discretization and its stabilization is briefly described for the sake of clarity and completeness.

#### 3.1 Time discretization

We consider a partition  $0 = t_0 < t_1 < \dots < T$ ,  $t_k = k\Delta t$ , with a time step  $\Delta t > 0$ , of the time interval  $(0, T)$  and approximate the solution  $\mathbf{v}(\cdot, t_n)$  and  $p(\cdot, t_n)$  (defined in  $\Omega_{t_n}$ ) at time  $t_n$  by  $\mathbf{v}^n$  and  $p^n$ , respectively. For the time discretization we employ a second-order two-step scheme using the computed approximate solution  $\mathbf{v}^{n-1}$  in  $\Omega_{t_{n-1}}$  and  $\mathbf{v}^n$  in  $\Omega_{t_n}$  for the calculation of  $\mathbf{v}^{n+1}$  in the domain  $\Omega_{t_{n+1}} = \Omega_{n+1}$ . We write

$$\frac{\partial \mathbf{v}}{\partial t}(x, t^{n+1}) \approx \frac{3\mathbf{v}^{n+1} - 4\hat{\mathbf{v}}^n + \hat{\mathbf{v}}^{n-1}}{2\Delta t} \quad \text{where } x \in \Omega_{n+1}, \quad (6)$$

where  $\hat{\mathbf{v}}^n$  and  $\hat{\mathbf{v}}^{n-1}$  are the approximate solutions  $\mathbf{v}^n$  and  $\mathbf{v}^{n-1}$  defined on  $\Omega_n$  and  $\Omega_{n-1}$ , respectively, and transformed onto  $\Omega_{n+1}$  with the aid of ALE mapping, i.e.  $\hat{\mathbf{v}}^i(x) = \mathbf{v}^i(\mathcal{A}_{t_i}(\xi))$  where  $x = \mathcal{A}_{t_{n+1}}(\xi) \in \Omega_{n+1}$ . Further, we approximate the domain velocity  $\mathbf{w}_D(x, t_{n+1})$  by  $\mathbf{w}_D^{n+1}$ , where

$$\mathbf{w}_D^{n+1}(x) = \frac{3\mathcal{A}_{t_{n+1}}(\xi) - 4\mathcal{A}_{t_n}(\xi) + \mathcal{A}_{t_{n-1}}(\xi)}{2\Delta t}, \quad x = \mathcal{A}_{t_{n+1}}(\xi), \quad x \in \Omega_{n+1}.$$

Then the time discretization leads to the following problem in domain  $\Omega_{n+1}$

$$\begin{aligned} \frac{3\mathbf{v}^{n+1} - 4\hat{\mathbf{v}}^n + \hat{\mathbf{v}}^{n-1}}{2\Delta t} - \nu \Delta \mathbf{v}^{n+1} + ((\mathbf{v}^{n+1} - \mathbf{w}_D^{n+1}) \cdot \nabla) \mathbf{v}^{n+1} + \nabla p^{n+1} &= 0, \\ \nabla \cdot \mathbf{v}^{n+1} &= 0, \end{aligned} \quad (7)$$

equipped with boundary conditions (4a-d) and the initial condition.

### 3.2 Weak formulation

For solution of the problem by finite element method, the time-discretized problem (7) is reformulated in a weak sense. The following notation is used: By  $W = \mathbf{H}^1(\Omega_{n+1})$  the velocity space is defined, by  $X$  the space of test functions is denoted

$$X = \{\varphi \in W : \varphi = 0 \text{ on } \Gamma_{Wt_{n+1}} \cap \Gamma_D\},$$

and by  $Q = L^2(\Omega_{n+1})$  the pressure space is denoted. Using the standard approach, cf. [18], the solution  $\mathbf{v} = \mathbf{v}^{n+1}$  and  $p = p^{n+1}$  of problem (7) satisfies

$$a(U, V) = f(V), \quad U = (\mathbf{v}, p) \quad (8)$$

for any  $V = (\mathbf{z}, q) \in X \times Q$ , where

$$\begin{aligned} a(U, V) &= \left( \frac{3}{2\Delta t} \mathbf{v}, \mathbf{z} \right) + \nu (\nabla \mathbf{v}, \nabla \mathbf{z}) + \mathcal{B}(\mathbf{v}, \mathbf{z}) + c_n(\mathbf{v}; \mathbf{v}, \mathbf{z}) - (p, \nabla \cdot \mathbf{z}) + (\nabla \cdot \mathbf{v}, q), \\ c_n(\mathbf{w}, \mathbf{v}, \mathbf{z}) &= \int_{\Omega_{n+1}} \left( \frac{1}{2} (\mathbf{w} \cdot \nabla \mathbf{v}) \cdot \mathbf{z} - \frac{1}{2} (\mathbf{w} \cdot \nabla \mathbf{z}) \cdot \mathbf{v} \right) dx - \left( (\mathbf{w}_D^{n+1} \cdot \nabla) \mathbf{v}, \mathbf{z} \right), \\ \mathcal{B}(\mathbf{v}, \mathbf{z}) &= \int_{\Gamma_I \cup \Gamma_O} \frac{1}{2} (\mathbf{v} \cdot \mathbf{n})^+ \mathbf{v} \cdot \mathbf{z} dS, \\ f(V) &= \frac{1}{2\Delta t} (4\hat{\mathbf{v}}^n - \hat{\mathbf{v}}^{n-1}, \mathbf{z}) - \int_{\Gamma_I} p_{ref}^i \mathbf{v} \cdot \mathbf{n} dS - \int_{\Gamma_O} p_{ref}^o \mathbf{v} \cdot \mathbf{n} dS, \end{aligned} \quad (9)$$

and by  $(\cdot, \cdot)$  we denote the scalar product in the space  $L^2(\Omega_{n+1})$ .

### 3.3 Spatial discretization

Further, the weak formulation (8) is approximated by the use of FEM: we restrict the couple of spaces  $(X, M)$  to finite element spaces  $(X_h, M_h)$ . First, the computational domain  $\Omega_t$  is assumed to be polygonal and approximated by an admissible triangulation  $\mathcal{T}_h$ , cf. [2]. Based on the triangulation  $\mathcal{T}_h$  the Taylor-Hood finite elements are used, i.e.

$$\begin{aligned} \mathcal{H}_h &= \{v \in C(\overline{\Omega_{n+1}}); v|_K \in P_2(K) \text{ for each } K \in \mathcal{T}_h\}, \\ \mathcal{W}_h &= [\mathcal{H}_h]^2, \quad X_h = \mathcal{W}_h \cap \mathcal{X}, \\ \mathcal{M}_h &= \{v \in C(\overline{\Omega_{n+1}}); v|_K \in P_1(K) \text{ for each } K \in \mathcal{T}_h\}. \end{aligned} \quad (10)$$

The couple  $(X_h, M_h)$  satisfy the Babuška-Brezzi inf-sup condition, which guarantees the stability of a scheme, cf. [20].

**Problem 1** (Galerkin approximations). *Find  $U_h = (\mathbf{v}_h, p_h) \in (X_h, M_h)$  such that  $\mathbf{v}_h$  satisfy boundary conditions (4a,b) and*

$$a(U_h, V_h) = f(V_h), \quad (11)$$

for all  $\mathbf{z}_h \in X_h$  and  $q_h \in M_h$ .

The Galerkin approximations are unstable in the case of high Reynolds numbers, when the convection dominates. In that case a stabilized method needs to be applied.

### 3.4 Stabilization

In order to overcome the above mentioned instability of the scheme, modified Galerkin Least Squares method is applied, cf. ([7]). We start with the definition of the local element rezidual terms  $\mathcal{R}_K^a$  and  $\mathcal{R}_K^f$  defined on the element  $K \in \mathcal{T}_h$  by

$$\mathcal{R}_K^a(\tilde{\mathbf{w}}; \mathbf{v}, p) = \frac{3\mathbf{v}}{2\Delta t} - \nu \Delta \mathbf{v} + (\tilde{\mathbf{w}} \cdot \nabla) \mathbf{v} + \nabla p, \quad \mathcal{R}_K^f(\hat{\mathbf{v}}_n, \hat{\mathbf{v}}_{n-1}) = \frac{4\hat{\mathbf{v}}_n - \hat{\mathbf{v}}_{n-1}}{2\Delta t}. \quad (12)$$

Further, the stabilizing terms are defined for  $U^* = (\mathbf{v}^*, p^*)$ ,  $U = (\mathbf{v}, p)$ ,  $V = (\mathbf{z}, q)$  by

$$\begin{aligned} \mathcal{L}_{GLS}(U^*; U, V) &= \sum_{K \in \mathcal{T}_h} \delta_K \left( \mathcal{R}_K^a(\tilde{\mathbf{w}}; \mathbf{v}, p), (\tilde{\mathbf{w}} \cdot \nabla) \mathbf{z} + \nabla q \right)_K, \\ \mathcal{F}_{GLS}(V_h) &= \sum_{K \in \mathcal{T}_h} \delta_K \left( \mathcal{R}_K^f(\hat{\mathbf{v}}_n, \hat{\mathbf{v}}_{n-1}), (\tilde{\mathbf{w}} \cdot \nabla) \mathbf{z} + \nabla q \right)_K, \end{aligned} \quad (13)$$

where the function  $\tilde{\mathbf{w}}$  stands for the transport velocity, i.e.  $\tilde{\mathbf{w}} = \mathbf{v}^* - \mathbf{w}_D^{n+1}$ . The additional grad-div stabilization terms read

$$\mathcal{P}_h(U, V) = \sum_{K \in \mathcal{T}_h} \tau_K (\nabla \cdot \mathbf{v}, \nabla \cdot \mathbf{z})_K.$$

In the case of bounded convection velocity the choice of parameters according [7] for BB stable pair of FE (reduced scheme) would be possible. However, in order to obtain a fast and efficient multigrid method, the following choice of the parameters  $\delta_K$  and  $\tau_K$  is used

$$\tau_K = \nu \left( 1 + Re^{loc} + \frac{h_K^2}{\nu \Delta t} \right), \quad \delta_K = \frac{h_K^2}{\tau_K},$$

where the local Reynolds number  $Re^{loc}$  is defined as  $Re^{loc} = \frac{h \|\mathbf{v}\|_K}{2\nu}$ .

**Problem 2** (Galerkin Least Squares stabilized approximations). *We define the discrete problem to find an approximate solution  $U_h = (\mathbf{v}_h, p_h) \in \mathcal{W}_h \times \mathcal{Q}_h$  such that  $\mathbf{v}_h$  satisfies approximately conditions (4a,b) and the identity*

$$a(U_h, V_h) + \mathcal{L}_{GLS}(U_h; U_h, V_h) + \mathcal{P}_h(U_h, V_h) = f(V_h) + \mathcal{F}_{GLS}(V_h), \quad (14)$$

for all  $V_h = (\mathbf{z}_h, q_h) \in \mathcal{X}_h \times \mathcal{Q}_h$ .

### 4 Multigrid solution of the linear system

The space-time discretized system (14) needs to be solved by some linearization scheme, e.g. by Oseen linearization procedure described e.g. in [18] or [19]. The solution of the linearized system (14) leads to the the solution of a modified saddle point system

$$S\underline{\mathbf{v}} + B\underline{p} = \underline{f}, \quad \tilde{B}^T \underline{\mathbf{v}} + \tilde{A}\underline{p} = 0, \quad (15)$$

where  $\underline{\mathbf{v}}$  and  $\underline{p}$  is the finite-dimensional representation of the finite element approximations of velocity and pressure, respectively. Let us mention that for the non-stabilized system (i.e. in the case of  $\delta_K \equiv \tau_K \equiv 0$ ) we have  $\tilde{A} = 0$  and  $\tilde{B} = B$ .

From the system of equations (15) the pressure degrees of freedoms can be formally eliminated by formally multiplying the first equation of (15) by  $\tilde{B}^T S^{-1}$  from the left, i.e. we get the system of equations

$$\left(\tilde{B}^T S^{-1} B - \tilde{A}\right) \underline{p} = \tilde{B}^T S^{-1} \underline{f}, \quad (16)$$

or with notation  $A_p = \tilde{B}^T S^{-1} B - \tilde{A}$  and  $g = \tilde{B}^T S^{-1} f$  we have

$$A_p \underline{p} = g,$$

which can be solved by the Richardson iterative method

$$\underline{p}^{(l+1)} = \underline{p}^{(l)} + C^{-1}(g - A_p \underline{p}^{(l)}), \quad (17)$$

where  $C$  is a suitable preconditioner, see e.g. [19]. Nevertheless the choice of the preconditioner  $C$  is complicated in the case of convection dominated flows and the convergence of the scheme (17) is in this case slow. Moreover the stabilizing terms also badly influences the convergence rates.

In many cases and for small number of unknowns, the system can be solved with the aid of a direct solver, which yields fast, efficient and robust scheme. We refer to direct solver UMFPACK, cf. [4], which in the cases studied by the authors up to now [18] was efficient for number of unknowns less then approximately  $10^5$ . However, with further increase of the number of unknowns the memory and CPU requirements grows too fast, so that the fast and efficient solution becomes impossible. One possibility is to use the parallel implementation of multi-frontal method, cf. [1].

Here, the solution of the system (15) is carried out by a simplified version of multi-grid method. Only single mesh and two levels of solution (coarse and fine grid levels) are used. The fine grid is represented by the used higher order finite elements (here Taylor-Hood finite elements, i.e. P2/P1 approximations for velocity/pressure). The coarse grid is considered as lower order finite elements (i.e. equal order P1/P1 approximations for velocity/pressure) The solution on the coarse grid can be obtained with the aid of direct solver UMFPACK, which was found to be fast enough in the studied cases. On the fine grid the multiplicative Vanka-type smoother is used, cf. [9], [10]. This approach (i.e. the direct solver on coarse grid and Vanka-type smoother on fine grid) resulted in an efficient and fast method, which can be easily implemented. The performance of the multigrid method was found to be excellent for the isotropic grids. In the case of anisotropic mesh refinement, the convergence rates nevertheless become worse. The proper solution in this case is subject of a further study.

## 5 Numerical results

In this section the numerical results for air flow in a symmetric two-dimensional channel are presented. The channel geometry described in [14] is employed here, see also Fig. 1.

### 5.1 Stationary solution

First, we consider the non-moving computational domain  $\Omega$ , where the influence of isotropically and anisotropically refined meshes is studied, see Fig. 2.

The following constants were used in the computations: fluid density  $\rho_\infty = 1.225 \text{ kg m}^{-3}$  and kinematic viscosity  $\nu = 1.5 \times 10^{-5} \text{ m}^2/\text{s}$ , the width of the inlet part of the channel is  $H = 0.0176 \text{ m}$ , the total length of the channel  $L = 0.16 \text{ m}$ , and the constant gap width  $g \equiv 4.4 \text{ mm}$ .

The boundary condition (4d) in the presented computations is replaced by the condition (5), where the constant flow velocity is prescribed  $\mathbf{v}_D(x, t) = (U_\infty, 0)^T$  at the inlet part of boundary  $\Gamma_I$ , and  $U_\infty$  was chosen in the range  $[0.01, 0.05] \text{ m s}^{-1}$ . The numerical results for stationary solution and different Reynolds numbers ( $Re = \frac{1}{8}LU_\infty/\nu$ ) are presented in Figs. 3-4, where the isolines of the magnitude of velocity are shown. The results computed on both meshes for same Reynolds numbers show that even for low Reynolds numbers several stationary symmetric and nonsymmetric solutions exist. Fig. 3 (left) shows the symmetric solution obtained on both meshes for  $Re = 20$ . For  $Re = 40$  and  $Re = 50$  in Figs. 3-4 on isotropic mesh the non-symmetric solution was obtained, whereas on the anisotropic symmetric mesh the solution remains symmetric. For higher Reynolds number  $Re > 50$  both solutions become non-symmetric.

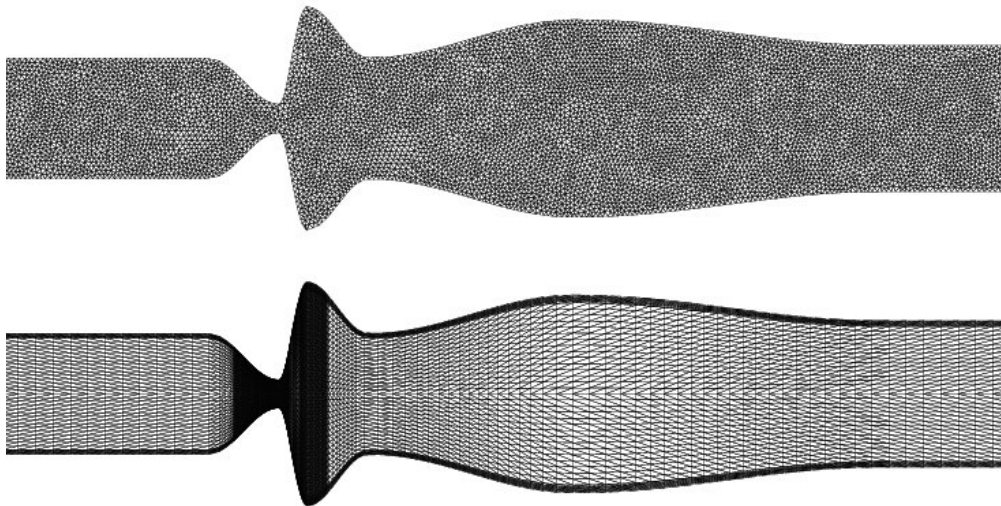


**Fig. 2:** *The employed grids: the isotropic non-symmetric mesh (upper part) with 12219 vertices and 23709 elements and approximately  $8 \times 10^4$  unknowns for flow problem, and the anisotropic axisymmetric mesh (lower part) with 8241 vertices and 16000 elements (resulting in  $6 \times 10^4$  unknowns).*

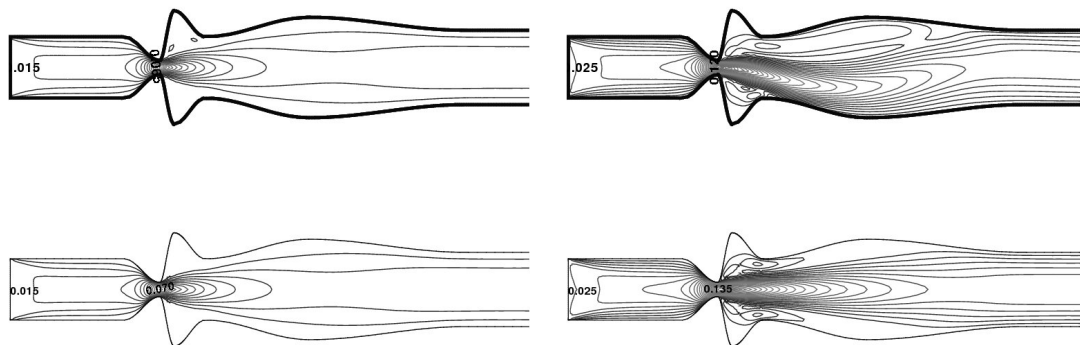


**Fig. 3:** *The isolines of flow velocity magnitudes for Reynolds number 20 (left) and 40 (right) on isotropic mesh(upper part) and anisotropic mesh (lower part).*

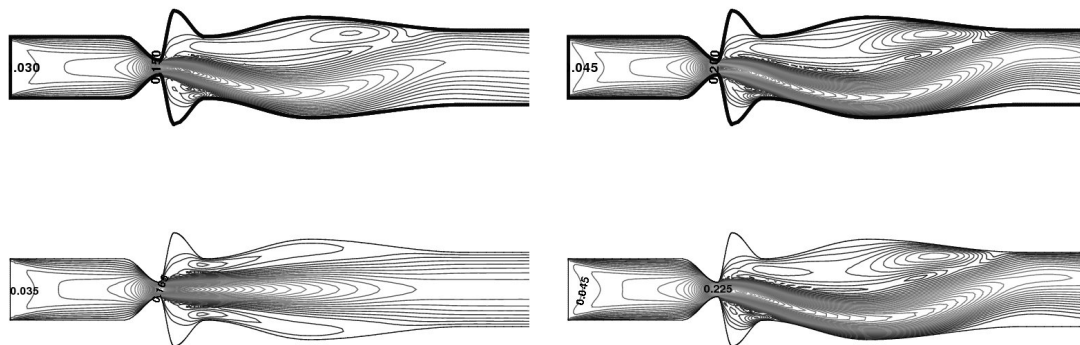


**Fig. 4:** *The isolines of flow velocity magnitudes for Reynolds number 50 (left) and 70 (right) on isotropic mesh(upper part) and anisotropic mesh (lower part).*

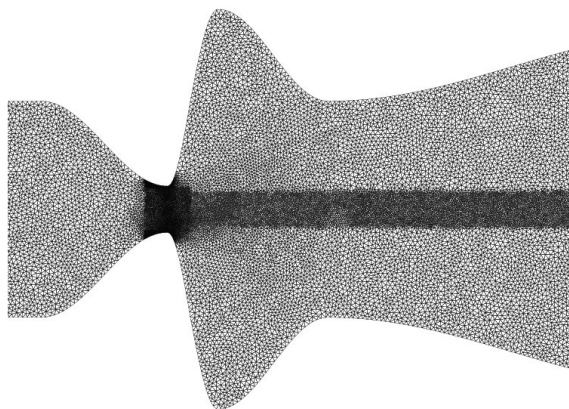


**Fig. 5:** *A detail of isotropic mesh used for multigrid solution with 42576 vertices and 84078 elements yielding approximately  $4 \times 10^5$  unknowns for the flow problem.*

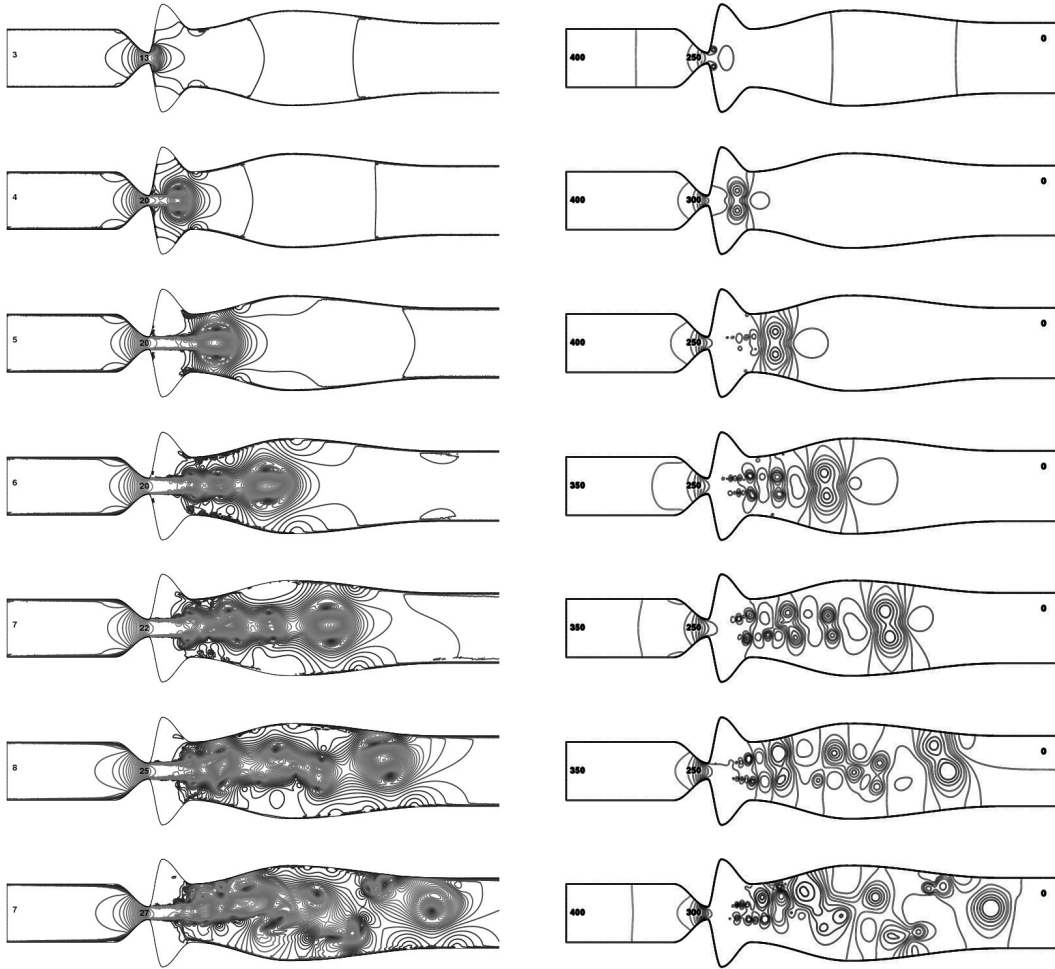


**Fig. 6:** The isolines of velocity magnitude (left) and pressure (right) in a sequence of time instance (from top to bottom, Part 1).

## 5.2 Flow in channel with vibrating vocal folds

The numerical results for flow in vibrating channel are presented for physically relevant pressure drop, inlet flow velocity, frequency of vibrations and width of the channel, which leads to the Reynolds numbers in the range  $Re = 1000 - 3000$ .

The computations were carried out for the pressure drop of 400 Pa, i.e.  $p_{ref}^i = 400$  Pa and  $p_{ref}^o = 0$  Pa. The initial condition was chosen as  $\mathbf{v}^0 \equiv 0$  and the isotropically refined mesh was used, cf. Fig. 5. The gap oscillates harmonically around the mean gap value  $\bar{g} = 4.4$  mm in the interval  $g(t) \in [3.2 \text{ mm}, 5.6 \text{ mm}]$  with frequency  $f = 100$  Hz .

The results are shown in Figs. 6-7 for the time instants marked in Fig. 8. The sudden expansion in the modelled glottal region leads to the faster flow in the vibrating narrowest part of the computational domain and to complicated flow structures in the outlet part of the channel. Similar effects were observed experimentally in [15].

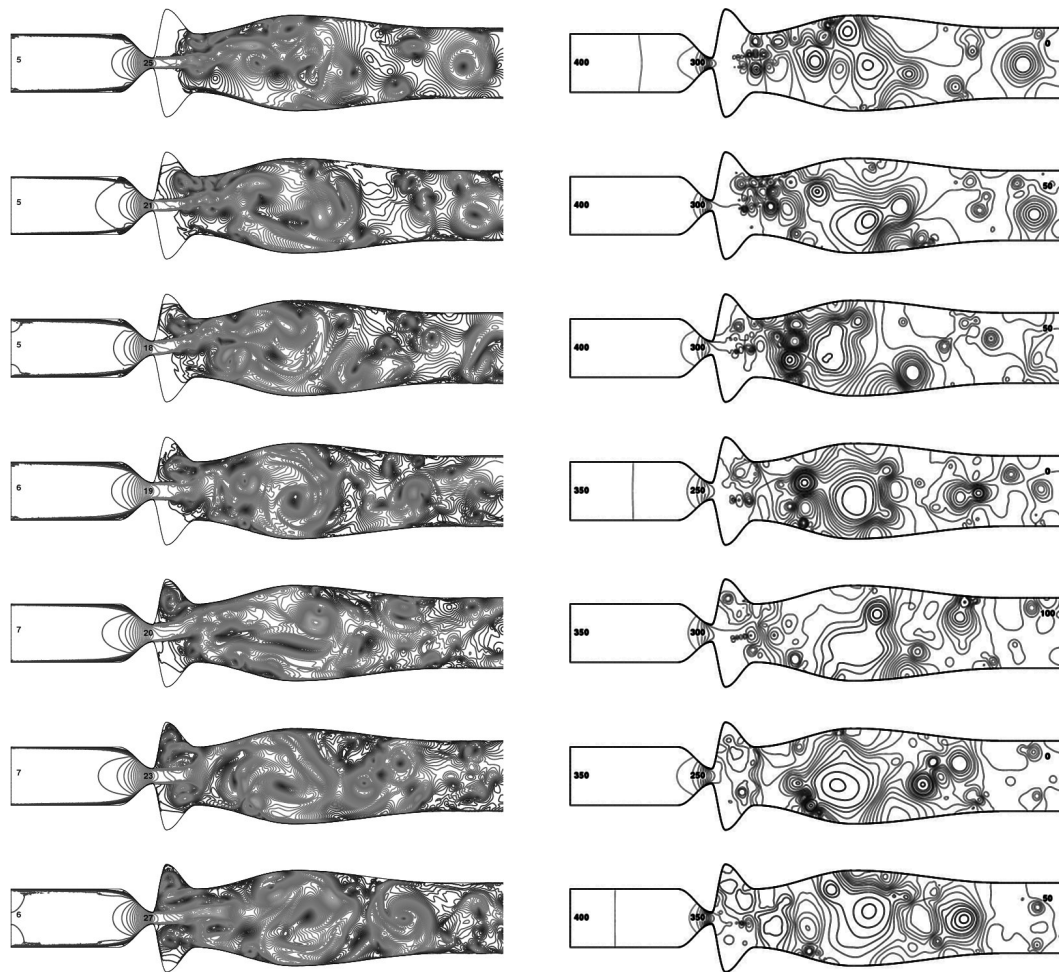


**Fig. 7:** *The isolines of velocity magnitude (left) and pressure (right) in a sequence of time instance (from top to bottom, Part 2).*

The inlet flow velocity and the flow velocity at on the axis of symmetry at the narrowest part of the channel are shown in Fig. 8. The both values oscillates with a similar frequency as the prescribed motion of the wall. However, the graphs are noisy partially due to the complicated flow structures downstream.

## 6 Conclusion

The paper presents the developed mathematical method and applied numerical technique for solution of fluid-structure problems encountered in biomechanics of voice production. The method consists of the advanced stabilization of the finite element method applied considering the moving domain. In order to obtain fast solution of the discretized problem a simplified multigrid method was applied, which allowed solution of significantly larger system of equations compared to the previously used approach, see e.g. [18].

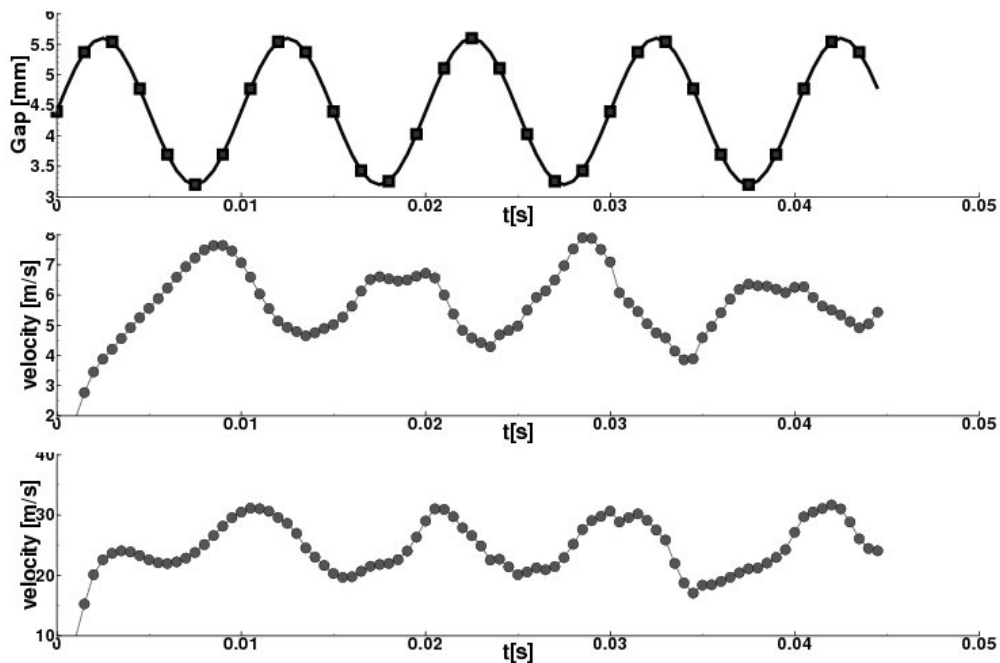


**Fig. 8:** The gap oscillations  $g(t)$  (upper graph), the computed flow velocity at the inlet (middle), and the computed flow velocity in the glottal orifice (lower graph).

The influence of the isotropic and anisotropic meshes was studied and the multi-grid technique was applied on a challenging problem of flow in symmetric channel with vibrating walls. The numerical results were presented showing the Coanda effect and complicated structure of small vortices and large size eddies generated at the glottal region by vibrating vocal fold. Similar vortex flow structures and Coanda effects were identified experimentally in [15].

## References

- [1] Amestoy, P.R., Guermouche, A., L'Excellent, J.Y., and Pralet, S.: Hybrid scheduling for the parallel solution of linear systems. *Parallel Computing* **32** (2006), 136–156.
- [2] Ciarlet, P.G.: *The finite element methods for elliptic problems*. North-Holland Publishing, 1979.
- [3] Codina, R.: Stabilization of incompressibility and convection through orthogonal sub-scales in finite element methods. *Computational Method in Applied Mechanical Engineering* **190** (2000), 1579–1599.
- [4] Davis, T.A. and Duff, I.S.: A combined unifrontal/multifrontal method for unsymmetric sparse matrices. *ACM Transactions on Mathematical Software* **25** (1999), 1–19.

- [5] Dolejší, V.: Anisotropic mesh adaptation technique for viscous flow simulation. *East-West Journal of Numerical Mathematics* **9** (2001), 1–24.
- [6] Feistauer, M.: *Mathematical methods in fluid dynamics*. Longman Scientific & Technical, Harlow, 1993.
- [7] Gelhard, T., Lube, G., Olshanskii, M.A., and Starcke, J.H.: Stabilized finite element schemes with LBB-stable elements for incompressible flows. *Journal of Computational and Applied Mathematics* **177** (2005), 243–267.
- [8] Heywood, J.G., Rannacher, R., and Turek, S.: Artificial boundaries and flux and pressure conditions for the incompressible Navier-Stokes equations. *Int. J. Numer. Math. Fluids* **22** (1992), 325–352.
- [9] John, V.: Higher order finite element methods and multigrid solvers in a benchmark problem for the 3D Navier-Stokes equations. *Int. J. Num. Meth. Fluids* **40** (2002), 775–798.
- [10] John, V. and Tobiska, L.: Numerical performance of smoothers in coupled multigrid methods for the parallel solution of the incompressible Navier–Stokes equations. *Int. J. Num. Meth. Fluids* **33** (2000), 453–473.
- [11] Nobile, F.: *Numerical approximation of fluid-structure interaction problems with application to haemodynamics*. Ph.D. thesis, Ecole Polytechnique Federale de Lausanne, 2001.
- [12] Nomura, T. and Hughes, T.J.R.: An arbitrary Lagrangian-Eulerian finite element method for interaction of fluid and a rigid body. *Computer Methods in Applied Mechanics and Engineering* **95** (1992), 115–138.
- [13] Otto, F.C. and Lube, G.: Non-overlapping domain decomposition applied to incompressible flow problems. *Contemporary Mathematics* **218** (1998), 507–514.
- [14] Punčochářová, P., Fürst, J., Kozel, K., and Horáček, J.: Numerical simulation of compressible flow with low mach number through oscillating glottis. In: Zolotarev, I., and Horáček, J. (Eds.), *Flow Induced Vibrations*. Institute of Thermomechanics, CAS, Prague, 2008 .
- [15] Šidlof, P.: *Fluid-structure interaction in human vocal folds*. Ph.D. thesis, Charles University, Faculty of Mathematics and Physics, 2007.
- [16] Sváček, P. and Feistauer, M.: Application of a stabilized FEM to problems of aeroelasticity. In: *Numerical Mathematics and Advanced Application*. Springer, Berlin, 2004 pp. 796–805.

- [17] Sváček, P., Feistauer, M., and Horáček, J.: Numerical simulation of a flow induced airfoil vibrations. In: *Proceedings Flow Induced Vibrations*, vol. 2. Ecole Polytechnique, Paris, 2004 pp. 57–62.
- [18] Sváček, P., Feistauer, M., and Horáček, J.: Numerical simulation of flow induced airfoil vibrations with large amplitudes. *Journal of Fluids and Structure* **23** (2007), 391–411.
- [19] Turek, S.: *Efficient solvers for incompressible flow problems: an algorithmic and computational approach*. Springer, Berlin, 1999.
- [20] Verfürth, R.: Error estimates for mixed finite element approximation of the Stokes equations. *R.A.I.R.O. Analyse numérique/Numerical analysis* **18** (1984), 175–182.